

verted to a polypeptide identical in size to the mature subunit (denoted OTC); a small portion was found as an intermediate-sized species (iOTC) whose precise physiologic significance remains unclear (3-6). When pOTC's programmed by *spf^{ash}/Y* RNA were processed, a far more complex pattern was observed (lane 4). Six distinct bands were noted, two each corresponding to mutant and normal pOTC's, iOTC's, and OTC's. These results were obtained with mitochondria from either control or mutant mice. Both mature-sized OTC species were found in mitochondrial fractions prepared from [³⁵S]methionine-labeled *spf^{ash}/Y* liver slices (not shown).

Finally, we asked whether both mature-sized OTC species observed with *spf^{ash}/Y* RNA can be assembled to trimeric form. After cell-free translation and mitochondrial processing, soluble products were applied to and eluted from a ligand affinity column (Fig. 3, legend) which, we have shown recently, binds only trimeric OTC composed of mature subunits (19). Significantly, only a single species was isolated from the *spf^{ash}/Y* programmed mixture (Fig. 3, lane 6), identical in mobility to that noted for the control (lane 5). This result strengthens our earlier finding (Fig. 1) that *spf^{ash}/Y* liver mitochondria contain only normal trimeric OTC.

We believe that the simplest hypothesis which accounts for these novel findings in *spf^{ash}/Y* mice is as follows. A mutation within the OTC structural gene creates an alternative intron-exon splice site similar to those observed for β -globin (20) or ovomucoid (21); the aberrant nuclear processing of pre-mRNA resulting therefrom leads to the formation of two distinct and translatable mRNA's; each mRNA directs the synthesis of a specific pOTC—one normal in size, the other elongated; both pOTC's are imported and processed by mitochondria but only the wild-type subunit is assembled to active trimeric enzyme. We cannot, however, exclude the possibility that the processed, mutant subunit undergoes assembly to homotrimeric, catalytically inactive enzyme that does not bind to the affinity ligand. Because we have recently succeeded in isolating a rat OTC complementary DNA (22), it should soon be possible to explore the mutation directly by analyzing mRNA and genomic DNA from *spf^{ash}/Y* mice.

LEON E. ROSENBERG
FRANTISEK KALOUSEK
MICHELLE D. ORSULAK

Department of Human Genetics,
Yale University School of Medicine,
New Haven, Connecticut 06510

References and Notes

1. L. E. Rosenberg and C. R. Scriver, in *Metabolic Control and Disease*, P. K. Bondy and L. E. Rosenberg, Eds. (Saunders, Philadelphia, ed. 8, 1980), p. 583; M. Walsler, in *The Metabolic Basis of Inherited Disease*, J. B. Stanbury, J. B. Wyngaarden, D. S. Fredrickson, J. L. Goldstein, M. S. Brown, Eds. (McGraw-Hill, New York, ed. 5, 1982), p. 402.
2. J. G. Conboy, F. Kalousek, L. E. Rosenberg, *Proc. Natl. Acad. Sci. U.S.A.* **76**, 5724 (1979); M. Mori, S. Miura, M. Tatibana, P. P. Cohen, *J. Biochem. (Tokyo)* **88**, 1829 (1980).
3. J. P. Kraus, J. G. Conboy, L. E. Rosenberg, *J. Biol. Chem.* **256**, 10739 (1981).
4. M. Mori, S. Miura, T. Morita, M. Takiguchi, M. Tatibana, *Mol. Cell. Biochem.* **49**, 97 (1982); S. Miura, M. Mori, M. Tatibana, *J. Biol. Chem.* **258**, 6671 (1983).
5. J. Conboy and L. E. Rosenberg, *Proc. Natl. Acad. Sci. U.S.A.* **78**, 3073 (1981); J. G. Conboy, W. A. Fenton, L. E. Rosenberg, *Biochem. Biophys. Res. Commun.* **105**, 1 (1982); D. M. Kolansky, J. G. Conboy, W. A. Fenton, L. E. Rosenberg, *J. Biol. Chem.* **257**, 8467 (1982).
6. C. Argan, C. J. Lusty, G. C. Shore, *J. Biol. Chem.* **258**, 6667 (1983).
7. R. DeMars, S. L. LeVan, B. L. Trend, L. B. Russell, *Proc. Natl. Acad. Sci. U.S.A.* **73**, 1693 (1976).
8. D. P. Doolittle, L. L. Hulbert, C. Cordy, *J. Hered.* **65**, 194 (1974).
9. P. Briand, B. Francois, D. Rabier, L. Cathelineau, *Biochim. Biophys. Acta* **704**, 100 (1982).
10. I. A. Qureshi, J. Letarte, R. Ouellet, in *Urea Cycle Diseases*, A. Lowenthal, A. Mori, B. Marescau, Eds. (Plenum, New York, 1982), p. 173.
11. P. Briand, L. Cathelineau, P. Kamoun, D. Gigot, M. Penninckx, *FEBS Lett.* **130**, 65 (1981).
12. The breeding pairs were kindly provided by Donald Doolittle. Mouse stock has been maintained since 1981 by crossing either *spf^{ash}/+* with *+Y* or *+/+* with *spf^{ash}/Y*. All mice were given free access to Wayne Lab Blox food supplemented periodically with oatmeal. Affected animals were identified 7 to 10 days after birth. The colony is now in its fifth generation.
13. F. Kalousek, B. Francois, L. E. Rosenberg, *J. Biol. Chem.* **253**, 3939 (1978).
14. G. Mancini, J. P. Vaerman, A. O. Carbonera, J. F. Heremans, in *Protein in Biological Fluids 11th Colloquium, Bruges*, H. Peeters, Ed. (Pergamon, Oxford, 1964), p. 370.
15. N. J. Hoogenraad, T. M. Sutherland, G. J. Howlett, *Anal. Biochem.* **101**, 97 (1980).
16. Native molecular weight, specific activity, p*H* optimum, and *K_m*s were determined as described (13). We determined the subunit molecular weight on 10 percent SDS-PAGE, using a Pharmacia low molecular weight calibration kit. The isoelectric point (pI) was determined by chromatofocusing, with the use of Polybuffer exchanger 94 and Polybuffer 96 from Pharmacia.
17. Y. W. Kan, in *The Metabolic Basis of Inherited Disease*, J. B. Stanbury, J. B. Wyngaarden, D. S. Fredrickson, J. L. Goldstein, M. S. Brown, Eds. (McGraw-Hill, New York, ed. 5, 1982), p. 1711.
18. We recognize that this result is an accurate quantitative reflection of translatable OTC mRNA only if the mutant and control RNA's and pOTC's are equally stable, and if the pOTC's have the same affinity for our antiserum to OTC.
19. F. Kalousek, M. D. Orsulak, L. E. Rosenberg, in preparation.
20. R. A. Spritz *et al.*, *Proc. Natl. Acad. Sci. U.S.A.* **78**, 2455 (1981); Y. Fukumaki *et al.*, *Cell* **28**, 585 (1982).
21. J. P. Stein, J. F. Catterall, P. Kristo, A. R. Means, B. W. O'Malley, *Cell* **21**, 681 (1980).
22. A. L. Horwich, J. P. Kraus, K. Williams, F. Kalousek, W. Konigsberg, L. E. Rosenberg, *Proc. Natl. Acad. Sci. U.S.A.* **80**, 4258 (1983).
23. This work was supported by grant AM 09527 from the National Institutes of Health. We thank E. Spector for providing us with *spf^{ash}* mice; P. Snodgrass for informing us of the *spf^{ash}* strain; R. Olsen for assistance with mouse care and breeding; W. Fenton, J. Kraus, and A. Horwich for useful discussion; and M. Feldman for secretarial assistance.

9 August 1983; revised 9 September 1983

Noninvasive Observations of Fluorinated Anesthetics in Rabbit Brain by Fluorine-19 Nuclear Magnetic Resonance

Abstract. Fluorinated anesthetics were observed noninvasively in the brain of intact rabbits with fluorine-19 nuclear magnetic resonance spectroscopy. High-resolution fluorine-19 spectra of halothane, methoxyflurane, and isoflurane were obtained with a surface coil centered over the calvarium. Elimination of halothane from the brain was also monitored by this technique. Residual fluorine-19 signals from halothane (or a metabolite) could be detected as long as 98 hours after termination of anesthesia. These observations demonstrate the feasibility of using this technique to study the fate of fluorinated anesthetics in live mammals.

It is generally believed that anesthesia is produced when an appropriate partial pressure of a volatile anesthetic agent is reached in the brain (1). Since only indirect methods have been available to study this phenomenon, information on the uptake and distribution of these agents in the brain has been extremely limited. Moreover, there is no information on the environments anesthetics occupy in the brain or on their residence times in this organ. Fluorinated hydrocarbons and ethers are among the most commonly used inhalation anesthetic agents. We used ¹⁹F nuclear magnetic resonance (NMR) spectroscopy to observe fluorinated anesthetic agents in the brain of a live mammal and monitored its uptake and elimination. In this technique the ¹⁹F

signals derived from the anesthetic molecule itself are used to detect its presence and to assess the environment in which the molecule resides. The approach is noninvasive, since ¹⁹F nuclei of the anesthetic molecule serve as the probe used to monitor the anesthetic-brain interaction.

We followed the incorporation of three different anesthetic agents into the rabbit brain (2): halothane (CF₃-CHBrCl), methoxyflurane (CHCl₂-CF₂-O-CH₃), and isoflurane (CF₃-CHCl-O-CF₂H). New Zealand White rabbits (3 to 4 kg) were subcutaneously injected with a combination of ketamine and xylazine, intubated (3), and positioned in the bore of the magnet. Each anesthetic agent was delivered with a "nonbreathing" system

involving intermittent positive-pressure ventilation and an individual precision vaporizer. Fluorine-19 spectra were acquired at 75.5 MHz by using a surface coil (4) on a spectrometer equipped with a 20-cm-bore superconducting magnet operating at 1.89 T. The surface coil was centered on the head over the calvarium, the optimum position for detecting ^{19}F signals from the brain. All chemical shifts were measured with respect to an external 1,2-dibromotetrafluoroethane standard.

Characteristic ^{19}F chemical shifts were observed for each of the anesthetic agents in the brain (Fig. 1). Halothane

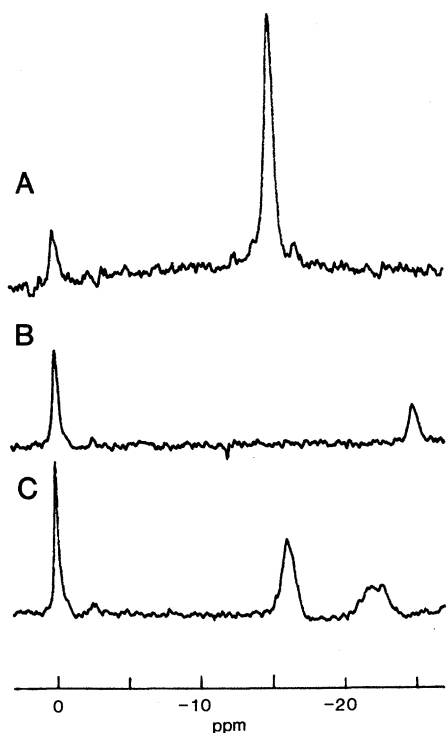


Fig. 1. Fluorine-19 NMR spectra of (A) halothane, (B) methoxyflurane, and (C) isoflurane. Three to five rabbits were studied for each anesthetic. Each animal was premedicated with ketamine (50 mg/kg) and xylazine (5 mg/kg), intubated, and positioned in the magnet. Subsequently, the rabbit was connected to an anesthesia machine and a background spectrum was taken before administration of the inhalation agent (1 percent halothane for 30 minutes, 1.5 percent methoxyflurane for 80 minutes, or 1 percent isoflurane for 40 minutes). Spectra were acquired on an Oxford Research Systems TMR-32 spectrometer with a surface coil (3.5 cm in diameter) placed on the frontal bones midway between the eyes. The following acquisition parameters were used: 5000-Hz sweep width, 0.41-second acquisition time, and 1200 transients; no proton decoupling was employed. The pulse widths used gave close to optimum signal-to-noise ratios per unit time. Standard resolution enhancement and digital filtering techniques were used in the data processing. Chemical shifts are reported relative to an external standard of 2.5 percent $\text{C}_2\text{Br}_2\text{F}_4$ in CHCl_3 (contained in a sealed 4-mm sphere) with ± 0.2 ppm accuracy.

and methoxyflurane each give a single resonance at -14.9 and -24.8 ppm, respectively. Isoflurane exhibits two signals, one at -16.1 ppm due to the trifluoromethyl group and the other at -22.4 ppm due to the difluoromethyl group. In the latter case ^1H - ^{19}F coupling on the order of 70 Hz is also observed. These chemical shifts reflect not only the chemical structure of the compound but also the microenvironment in which the fluorine nucleus resides (5). The observed signals were shifted downfield, relative to those of pure anesthetics, by 1.0 ppm for halothane, 0.6 ppm for methoxyflurane, and 4.0 ppm for isoflurane. These are sizable shifts when compared to the shifts of 2.2 to 2.8 ppm observed for these compounds in different solvents. The relatively narrow lines (50 to 70 Hz) observed for these anesthetics suggest that they possess a fair amount of mobility in the environments in which they reside. By comparing these observations with spectra of the anesthetics in excised muscle and nerve (6) as well as in pure solvents (7), we conclude that the average environment of the anesthetic in the brain is not entirely lipophilic but has a polar character as well. This is consistent with the observation that the anesthetic potencies of the compounds studied are well correlated with their octanol/water partition coefficients and poorly correlated with their alkane/water partition coefficients (8).

We also followed the time course of halothane elimination from the rabbit brain (Fig. 2). After 30 minutes of 1 percent halothane anesthesia, administration of the anesthetic was stopped and the halothane concentration in the brain was monitored as this agent was removed from the body in the expired air. During the first 7 hours the halothane level declined to only 40 percent of the maximum value. Further decreases were observed after longer elapsed times: at 24 hours the level was 30 percent of the maximum value, and at 98 hours, 20 percent. The ^{19}F chemical shift of the halothane signal was constant through the first 7 hours of observation and subsequently showed a downfield shift of approximately 1 ppm.

These results were confirmed by studying brain samples excised from animals killed at intervals after halothane anesthesia was ended. The same trend in anesthetic concentration was observed. Furthermore, the downfield shift of 1 ppm seen in the living animal was also observed in the brains of rabbits killed 9 hours and longer after anesthesia. The presence of halothane in the excised tissues was verified by mass spectrometry.

The volatile halothane continues to evaporate from a tissue sample placed in the vacuum chamber of a mass spectrometer for up to 48 hours after anesthesia. No halothane was found by this method after longer intervals, although its presence (or that of a metabolite) continued to be demonstrated in the tissue by the (shifted) ^{19}F signal. It has generally been assumed that halothane elimination from the brain would be complete within a few hours after administration of this agent is discontinued. However, there have been no direct in vivo measurements of halothane levels in the brain over long periods of time. Thus this demonstration of the presence of a significant amount of halothane or a halothane metabolite in brain tissue for as long as 98 hours after anesthesia is a surprising result.

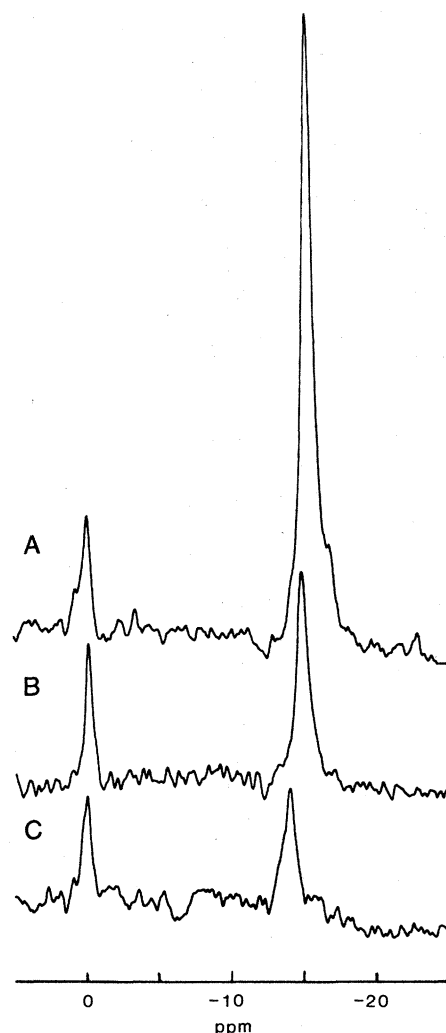


Fig. 2. Fluorine-19 NMR spectra of halothane in a rabbit brain (A) immediately after, (B) 7 hours after, and (C) 98 hours after 30 minutes of exposure to 1 percent halothane. After administration of the inhalation agent was terminated, anesthesia was maintained with injections of ketamine and xylazine. Spectra were collected and processed under the same conditions described in the legend to Fig. 1.

From the chemical shift data, it can be concluded that the compound that survives in the brain for at least 98 hours has retained the intact CF₃ group of the halothane molecule. Furthermore, there is no major change in the brain environment in which this molecule resides over this period. The long retention time suggests either the presence of a covalently bound halothane or conversion to a less volatile metabolite. Either possibility would be consistent with our preliminary mass spectrometric data. At this time we are unable to assign a structure to the long-lived species in the brain, although the ¹⁹F NMR observation of a similar compound in blood, nerve, and muscle strongly suggests a nonvolatile species that can easily cross cell membranes.

In conclusion, we have directly observed the interaction of general anesthetics with brain tissue in a live mammal. We showed that by using ¹⁹F NMR spectroscopy, one can detect small concentrations (100 to 500 μM) of fluorinated anesthetics in the brain during and after anesthesia. Spectra with good signal-to-noise ratios were obtained at 2-minute intervals, so it should be possible to follow the time course of anesthetic uptake and elimination as well as to detect the appearance of fluorine-containing metabolites in various organs in vivo over relatively short periods.

ALICE M. WYRWICZ*

MARGARET H. PSZENNY

Department of Chemistry,

University of Illinois, Chicago 60680

JOHN C. SCHOFIELD

Biological Resources Laboratory,

University of Illinois, Chicago

PHILIP C. TILLMAN

Animal Resources Service,

School of Veterinary Medicine,

University of California, Davis 95616

ROY E. GORDON

PETER A. MARTIN

Oxford Research Systems,

Abingdon OX14 1RY, England

References and Notes

1. G. Merkel and E. I. Eger, *Anesthesiology* **24**, 346 (1963); E. I. Eger, *Anesthetic Uptake and Action* (Williams & Wilkins, Baltimore, 1974), pp. 77-95; B. R. Fink, *Anesthesiology* **34**, 403 (1971).
2. Control experiments were performed in which the surface coil was placed directly on the surgically exposed frontal bones prepared under general anesthesia. The same results were obtained, confirming that the major source of the ¹⁹F NMR signals was the brain. Examination of the scalp and other intervening tissues showed negligible amounts of ¹⁹F signals.
3. D. J. Alexander and G. C. Clark, *Lab. Anim. Sci.* **30**, 871 (1980).
4. J. J. H. Ackerman *et al.*, *Nature (London)* **283**, 167 (1980).
5. J. T. Gerig, in *Biological Magnetic Resonance*, L. Berliner and J. Reuben, Eds. (Plenum, New York, 1978), vol. 1, pp. 139-188; W. E. Hull and B. D. Sykes, *Biochemistry* **15**, 1535 (1976).
6. A. M. Wyrwicz, Y. E. Li, J. C. Schofield, C. T. Burt, *FEBS Lett.*, in press.

7. L. S. Koehler, W. Curley, K. A. Koehler, *Mol. Pharmacol.* **13**, 113, (1976); K. A. Koehler *et al.*, *J. Magn. Res.* **30**, 75 (1978).
8. N. P. Franks and W. R. Lieb, *Nature (London)* **274**, 339 (1978); Y. Katz and S. A. Simon, *Biochim. Biophys. Acta* **471**, 1 (1977).
9. This work was carried out by using TMR-32 spectrometers at Oxford Research Systems, Oxford, England, and at the Biological Chemistry

Department, University of California, Davis. We thank E. M. Bradbury for his support. Supported in part by NIH grant GM 29520 and by NIH research career development award K04 GM 00503 to A.M.W.

* To whom requests for reprints should be addressed.

4 May 1983; revised 29 July 1983

Identification of the *c-myc* Oncogene Product in Normal and Malignant B Cells

Abstract. *Antiserum to a synthetic peptide corresponding to the carboxyl-terminus of the human c-myc protein immunoprecipitated a 48,000-dalton protein from a number of normal and malignant human and mouse cells. The size of the protein is consistent with the potential coding region predicted from the c-myc nucleotide sequence, and is the same for malignant cells carrying either a rearranged or an unrearranged c-myc oncogene. Because c-myc transcripts are expressed at higher levels in malignant than in normal B cells, it appears that an increased level of the c-myc protein rather than a change in the gene product is the relevant factor in determining transformation.*

The human cellular homolog (*c-myc*) of the avian MC-29 viral transforming gene is normally located on band q24 of chromosome 8 (1, 2). In Burkitt lymphoma, the translocation involving chromosomes 8 and 14 [t(8;14)] (3) brings the *c-myc* gene in close proximity with the immunoglobulin heavy chain locus on chromosome 14 (1). We have previously found that the translocated *c-myc* gene in Burkitt lymphomas is either not rearranged, or rearranged head to head with the immunoglobulin constant region C_μ gene (1, 4).

The *c-myc* transcripts are expressed at higher levels in Burkitt lymphoma cells than in lymphoblastoid cells not carrying the translocation (5, 6). From further studies using somatic hybrids between mouse myeloma and Burkitt lymphoma cells carrying the chromosome with either the translocated or the untranslocated *c-myc* gene, and Burkitt cell lines carrying rearranged and unrearranged *c-myc* genes, we concluded that only the translocated gene is expressed in Burkitt lymphoma cells (6, 7). In all the cases examined, the length of the *c-myc* transcripts was approximately 2.3 kb (5-7).

In mouse plasmacytoma, the *c-myc* gene, which normally resides on chromosome 15, is translocated to the immunoglobulin heavy chain locus on chromosome 12 (8, 9). Mouse plasmacytomas in which the *c-myc* gene recombines with the C_α gene express novel 1.9- to 2.1-kb *myc* transcripts that are 0.4 kb shorter than the normal cellular *myc* transcripts (8, 9). The levels of *c-myc* transcripts are also elevated in mouse plasmacytoma (8).

The increased levels of *c-myc* transcripts in Burkitt lymphoma cells and

mouse plasmacytomas suggest a possible role in transformation for the protein encoded by this oncogene. Therefore, we attempted to detect the *c-myc* product using antiserum to a synthetic peptide that corresponds to the carboxyl-terminus of the predicted protein (10, 11). Figure 1 shows the structure of the synthetic peptide and the corresponding protein sequence of human *c-myc* (10, 11). This peptide, prepared by the Merrifield solid-phase method (12), has 12 amino acids, with a tyrosine residue added at the amino end for coupling with the bovine serum albumin (BSA) carrier (13).

Rabbits were injected with the peptide-BSA conjugate, and given booster injections at 2-week intervals. Blood was withdrawn after the fourth booster injection. The antiserum thus obtained was assayed for the presence of antibodies to the *myc* gene product by immunoprecipitation of [³⁵S]methionine-labeled extracts of Burkitt lymphoma cells and human cell lines positive for *c-myc* transcripts by Northern blot or S1 nuclease analysis (5-7). The precipitates were analyzed by sodium dodecyl sulfate (SDS)-polyacrylamide gels (14), with serum from nonimmunized rabbits (preimmune serum) being used as a control. Immunoprecipitation inhibition experiments were carried out with antiserum that had been incubated with uncoupled peptide (10⁻³M) to confirm that the amino acid sequence detected by the antibodies was the same as that of the peptide used for immunization.

The antiserum to the terminal peptide precipitated a 48,000-dalton polypeptide from Daudi, P3HR1, and JD38 IV lymphoma cells (Fig. 2A, lanes 2, 5, and 7,